

# Layer-by-layer Deposition of TiO<sub>2</sub> Nanoparticles in the Wood Surface and its Superhydrophobic Performance

Xi Lu and Yingcheng Hu \*

A hydrophilic wood surface was transformed to become superhydrophobic by layer-by-layer (LbL) assembly of polyelectrolyte/titanium dioxide (TiO<sub>2</sub>) nanoparticles multilayers and subsequent hydrophobic modification with 1H, 1H, 2H, 2H-perfluoroalkyltriethoxysilane (POTS). The chemical composition of the wood samples before and after treatment was characterized by energy dispersive X-ray analysis (EDXA), Fourier transform infrared spectroscopy (FTIR), X-ray diffraction (XRD), and thermogravimetric analysis (TGA). These analyses showed that a high-surface-roughness film of TiO<sub>2</sub> nanoparticles deposited by LbL became combined on the wood surface with a low-surface-energy thin layer of POTS. The microstructure and the hydrophobicity of the wood samples were analyzed by scanning electron microscope (SEM) and contact angle measurements, respectively. The morphology and the values of water contact angle (WCA) demonstrated that the reaction pH and number of self-assembled layers were the main factors affecting hydrophobic wood samples. After assembly with 5 or more multilayers, the wood surface exhibited excellent superhydrophobicity with the highest WCA of 161°.

*Keywords:* Superhydrophobic; Wood surface; Layer-by-layer assembly; TiO<sub>2</sub> nanoparticles

*Contact information:* Key Laboratory of Bio-based Material Science and Technology of Ministry of Education of China, College of Material Science and Engineering, Northeast Forestry University, Harbin, China; \*Corresponding author: yingchenghu@163.com

## INTRODUCTION

As a natural composite, wood is mainly composed of cellulose, hemicellulose, and lignin; the cellulose and hemicellulose molecules have many hydrophilic hydroxyl (-OH) groups (Wang *et al.* 2011a). Wood is very sensitive to moisture, and in many applications its instability in changing moisture conditions is a major disadvantage compared with other materials. Wood properties can be improved considerably by converting hydrophilic -OH groups into more hydrophobic groups. With new methods for synthesizing and preparing nanomaterials, superhydrophobic materials are of great interest because of their unique wettability and development potential. A superhydrophobic surface is defined as one that has a water contact angle (WCA) greater than 150° when water droplets are placed on the surface. One of the most well-known examples of superhydrophobic surfaces in nature is the lotus leaf (Wang *et al.* 2012; Dai *et al.* 2013). A superhydrophobic surface can be prepared by a combination of a high-surface-roughness film and a low-surface-energy thin layer (Wang *et al.* 2011b; Wan *et al.* 2014; Zheng *et al.* 2015). Gao reported a two-step method for the preparation of a superhydrophobic film on wood surface which consists of fabricating a TiO<sub>2</sub> film through a low-temperature hydrothermal method and subsequent modification by (heptadecafluoro-1,1,2,2-tetradecyl) trimethoxysilane (Gao *et al.* 2015a). However, using a layer-by-layer (LbL) assembly technique to fabricate superhydrophobic wood has not yet been reported.

The electrostatic LbL assembly technique is appealing because it is simple, general, and does not require complex or expensive instruments (Decher 1997). Film formation is controlled by adjusting the conditions of adsorption (Zhang *et al.* 2004). In LbL assembly, polycations and polyanions are alternately deposited to form a multilayer film on solid surfaces through electrostatic interactions (Elosua *et al.* 2013). A variety of functional substances including polyelectrolytes (Sundman and Laine 2013), inorganic nanoparticles (Li *et al.* 2013), chitosan (Fang *et al.* 2015), and enzyme (Xing *et al.* 2007) have been employed to fabricate LbL multilayer films. Polyelectrolyte/polyelectrolyte or polyelectrolyte/nanoparticles multilayers created by LbL assembly can also be deposited on wood (Lin *et al.* 2008; Renneckar and Zhou 2009). The modified fibers have improved physical properties and special functionalities such as high scalability (Marais *et al.* 2014), high porosity (Lu *et al.* 2007), electroconductibility (Agarwal *et al.* 2009), magnetism (Cranston and Gray 2006), flame resistance (Laufer *et al.* 2012), superhydrophobicity, (Zhang *et al.* 2012a) *etc.* (Zhou *et al.* 2010; Zamarreño *et al.* 2011).

This study used the LbL assembly technique to control the deposition of TiO<sub>2</sub> nanoparticles on wood. The reaction pH values were varied, and self-assembled layers that contained a chemisorbed monolayer of 1H, 1H, 2H, 2H-perfluorooctyltriethoxysilane (POTS) reagent combined to make a superhydrophobic surface. The prepared hydrophobic wood surfaces were characterized *via* energy dispersive X-ray analysis (EDXA), Fourier transform infrared (FTIR) spectroscopy, X-ray diffraction (XRD), thermogravimetric analysis (TGA), and scanning electron microscopy (SEM). The hydrophobicity of the treated samples was measured by contact angle (CA) measurements. This article provides a new approach to preparing superhydrophobic wood, which has far-reaching consequences.

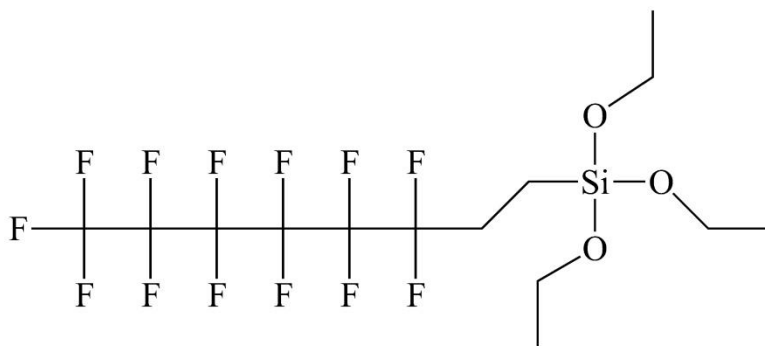


Fig. 1. Molecular structure of 1H, 1H, 2H, 2H-perfluorooctyltriethoxysilane

## EXPERIMENTAL

### Materials

Poplar wood (*Populus tomentosa*) was cut into 20 mm (tangential) × 20 mm (radial) × 20 mm (longitudinal) pieces that were ultrasonically rinsed in acetone for 30 min and dried in vacuum at 80 °C for 24 h. Linear sodium poly(styrenesulfonate) (PSS, *M<sub>w</sub>* of 70000) and branched pol (ethylenimine) (PEI, *M<sub>w</sub>* of 25000) were obtained from Sigma Aldrich (Shanghai, China). The TiO<sub>2</sub> nanoparticles (anatase) with a diameter range of 20 to 80 nm and 1H, 1H, 2H, 2H-perfluorooctyltriethoxysilane (POTS; 97%; Fig. 1) were purchased from Aladdin Industrial Corporation (Shanghai, China). Ultrapure water was produced in-house. All chemicals were used as received without further purification.

## Methods

### *Preparation of TiO<sub>2</sub> nanoparticles on the wood surface by the LbL assembly technique*

The preparation conditions are shown in Table 1. The wood samples were immersed separately into solutions of PEI (10 mg/mL) and PSS (1 mg/mL) to form a PEI/PSS bilayer on the wood surface, after which nanoparticle-containing (PSS/TiO<sub>2</sub>)<sub>n</sub> (n = 1, 3, 5, 7, 9) multilayers were assembled by alternately immersing the wood samples into PSS solution and a solution containing TiO<sub>2</sub> nanoparticles (4 mg/mL). These three solutions were adjusted to different pH values. For each layer, the sample was immersed separately in 100 mL of stirred polyelectrolyte/TiO<sub>2</sub> nanoparticle solutions for 40 min and washed three times with ultrapure water for 20 min between each deposited layer. By repeating these steps, a thin film of PEI(PSS/TiO<sub>2</sub>)<sub>n</sub> multilayers was fabricated on the wood surface. The coating was terminated with TiO<sub>2</sub> nanoparticles on the outermost layer.

**Table 1.** Synthetic Conditions for Growing TiO<sub>2</sub> on Wood Surfaces

Samples	pH(PEI)	pH(PSS)	pH(TiO <sub>2</sub> )	n	Mean (°)	WCA	
						SD	CV (%)
S1	10.5	6	6	1	133	2.7	2.0
S2	10.5	6	6	3	142	1.8	1.3
S3	10.5	6	6	5	153	1.1	0.7
S4	10.5	6	6	7	156	1.2	0.8
S5	10.5	6	6	9	161	2.0	1.2
S6	10	6	8	5	148	1.0	0.7
S7	10	6	6	5	152	1.0	0.6
S8	10	8	8	5	141	1.2	0.9
S9	10	8	6	5	145	1.1	0.7
S10	6	8	8	5	121	1.1	0.9
S11	6	8	6	5	128	1.4	1.0
S12	6	6	8	5	131	1.6	1.2
S13	6	6	6	5	135	1.5	1.1

SD: Standard Deviation; CV: Coefficient of Variation

### *Modification of TiO<sub>2</sub>-coated wood by POTS*

The TiO<sub>2</sub>-coated wood samples were modified by POTS using vapor-phase deposition. Briefly, the TiO<sub>2</sub>-coated wood samples were immersed in a small sealed container with 2.0 wt% POTS reagent in methyl alcohol solution at 90 °C for 12 h so that the POTS molecules would completely react with the surface -OH groups of TiO<sub>2</sub>. Finally, POTS-modified wood samples were rinsed with ethyl alcohol to remove residual chemicals and dried in the oven at 60 °C for 24 h under nitrogen (N<sub>2</sub>) flow.

## Characterization

The chemical composition of the wood samples before and after treatment was characterized by EDXA (GENESIS 2000 XMS, EDAX, Mahwah, NJ, USA). FTIR spectra were collected with a Nicolet Magna-IR 560 spectrometer (Thermo Fisher Scientific, Waltham, MA, USA) with a resolution of 4 cm<sup>-1</sup>, scanning range of 4000 to 500 cm<sup>-1</sup>, and 32 scans. The crystallization patterns were analyzed by D/MAX 220 X-ray diffractometer (Rigaku Corporation, Tokyo, Japan) with Ni-filtered Cu K $\alpha$  radiation ( $\lambda = 1.5418 \text{ \AA}$ ) at a scan rate of 4° min<sup>-1</sup> and a scanning angle ( $2\theta$ ) ranging from 5° to 70°. The measurement conditions included an accelerating voltage of 40 kV, applied current of 30 mA, and progressive scanning step width of 0.02°. TGA was conducted on a simultaneous thermal analyzer (STA6000TGA, PerkinElmer, Waltham, MA, USA) from 25 to 700 °C at a

heating rate of 10 °C/min under a N<sub>2</sub> atmosphere. The samples were cut from wood wafers to the size of 5 × 5 × 5 mm<sup>3</sup>, and the surface morphology was analyzed with SEM (Quanta200, FEI, Hillsboro, OR, USA) at an acceleration voltage of 12.5 kV. WCA was measured using an OCA20 CA analyzer (Data Physics, Filderstadt, Germany) at room temperature with a 5 µL droplet of deionized water and a dose rate of 0.5 µL s<sup>-1</sup>. For each WCA measurement, five different locations were randomly selected on the radial section, and the average value was recorded. The environmental stability was evaluated by immersing in ultrapure water and testing WCAs change over time. The environmental durability was performed by placing the samples in the interior and a WCA test every five days.

## RESULTS AND DISCUSSION

### EDXA Spectrum

The EDXA spectrum of the wood samples before and after the LbL assembly process is shown in Fig. 2. The main wood components were carbon and oxygen. EDXA cannot detect hydrogen, and the gold element was derived from sputtering the wood surface prior to SEM. In the self-assembled wood specimens, a strong absorption peak at approximately 4.6 keV was the Ti atom absorption peak, indicating the presence of TiO<sub>2</sub> nanoparticles on the wood surface. The amount of TiO<sub>2</sub> nanoparticles deposited on the wood surface increased from 6.77% to 14.79% when PEI(PSS/TiO<sub>2</sub>)<sub>n</sub> multilayers were increased from 1 to 9 (S1 to S5).

### FTIR Spectra

Figure 3 shows the FTIR spectra of an untreated specimen (a), specimens assembled with PEI(PSS/TiO<sub>2</sub>)<sub>n</sub> multilayers (b through d), and TiO<sub>2</sub> nanoparticles (e). With the addition of 1 layer, the stretching vibrations absorption peak of the -OH groups at the absorption band of 3389 cm<sup>-1</sup> became less evident. This result suggests that the decrease of the -OH stretching signal in IR could be due to the formation of layers. Because IR signals are depth-dependent, it means that as the LbL procedure is continued, the signals corresponding to the cellulose eventually fade due to the penetration depth of the IR radiation. The strong absorption band at 578 cm<sup>-1</sup> in the FTIR spectra of the self-assembled wood specimens was related to the Ti-O-Ti stretch vibration peak (Colomer and Velasco 2007), indicating that TiO<sub>2</sub> nanoparticles were successfully deposited on the wood surface. The absorption peak at 1113 cm<sup>-1</sup> was attributed to the Si-O-Ti symmetric stretching vibration (Chandrasekhar *et al.* 1980) originating from the Si-OH groups of POTS molecules attached to surface -OH groups of TiO<sub>2</sub> nanoparticles (Razmjou *et al.* 2012). The absorption bands located from 1300 to 1000 cm<sup>-1</sup> were due to the -CF<sub>3</sub>, -CF<sub>2</sub>, and Si-C absorption peaks of POTS molecules (Wang *et al.* 2011c), which overlapped the strong absorption peak of Si-O-Ti symmetric stretching vibration. Eventually, it was demonstrated that the modified POTS molecules were combined with the assembled TiO<sub>2</sub> nanoparticles on the wood surface, which lowered the surface energy of TiO<sub>2</sub> nanoparticle coatings. These generated groups demonstrated that superhydrophobic wood had been successfully prepared by LbL assembly *via* the mechanism shown in Fig. 4.

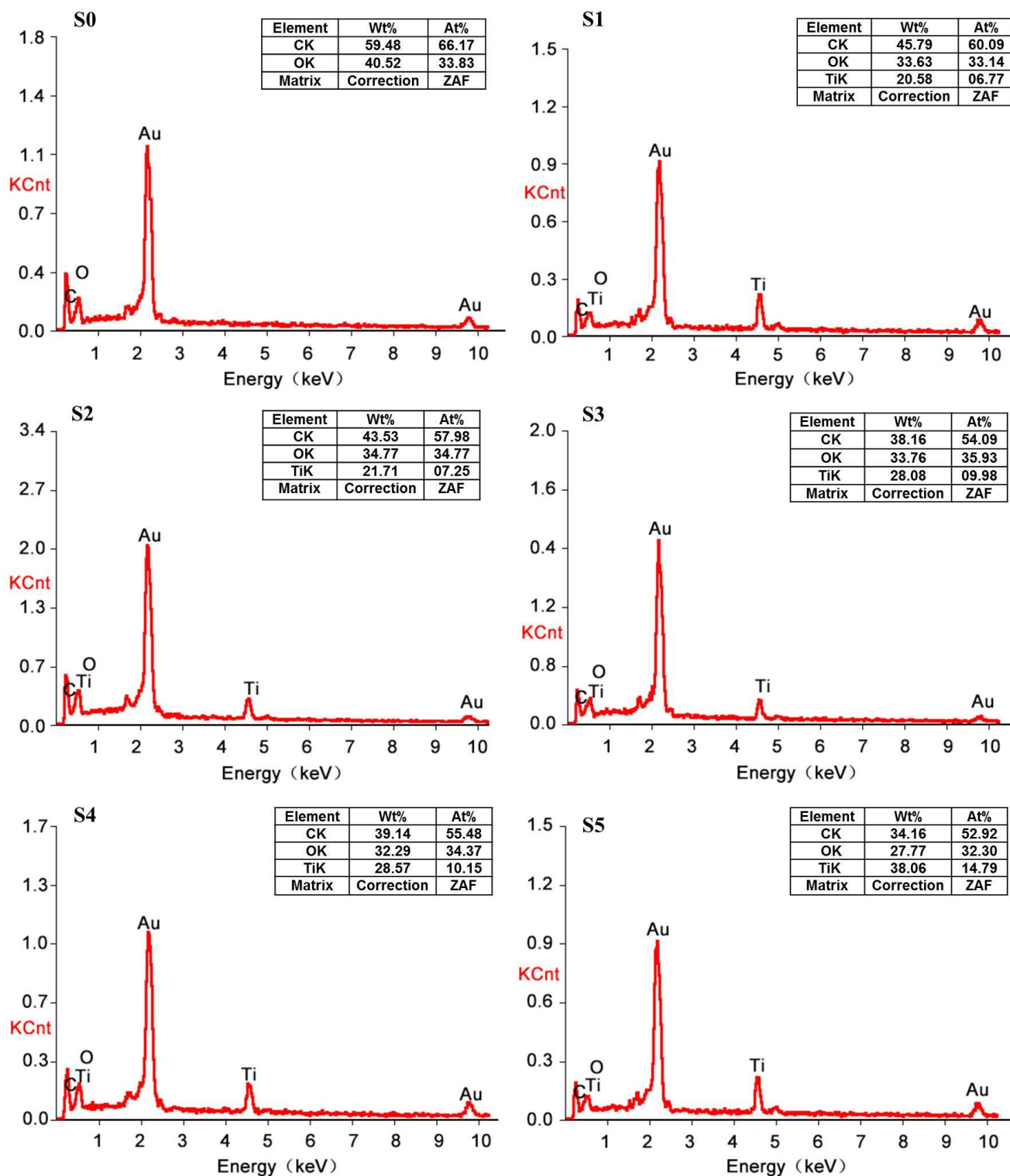


**Fig. 2.** The EDXA spectra of control specimen (S0) and specimens assembled with PEI(PSS/TiO<sub>2</sub>)<sub>n</sub> multilayers: (S1) n = 1, (S2) n = 3, (S3) n = 5, (S4) n = 7, and (S5) n = 9

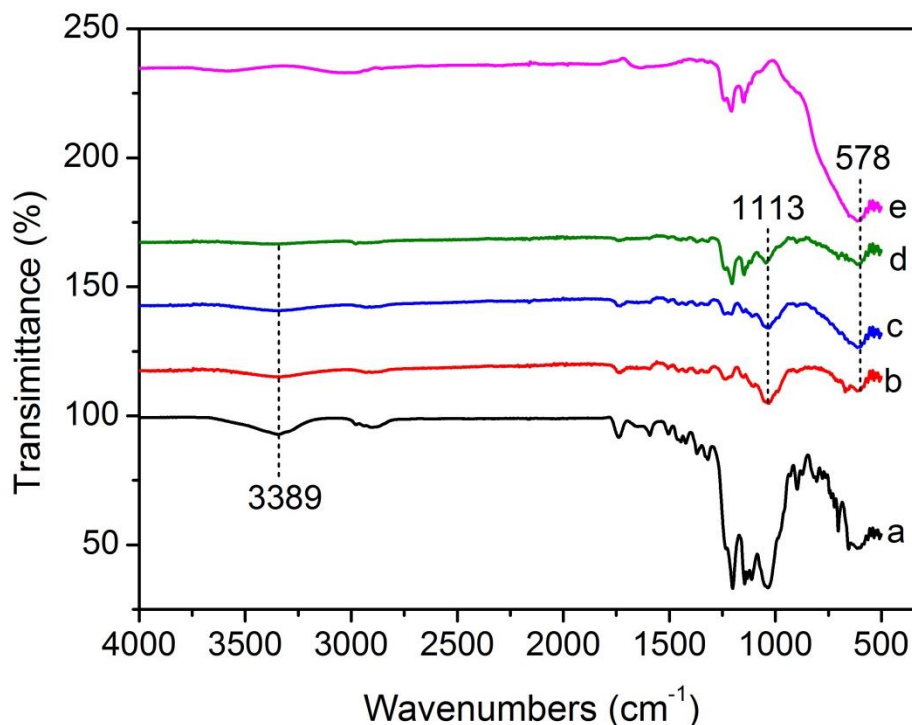


**Fig. 3.** FTIR spectra of (a) untreated specimen and specimens assembled with PEI(PSS/TiO<sub>2</sub>)<sub>n</sub> multilayers: (b) n = 1, (c) n = 3, (d) n = 5, and (e) nano-TiO<sub>2</sub>

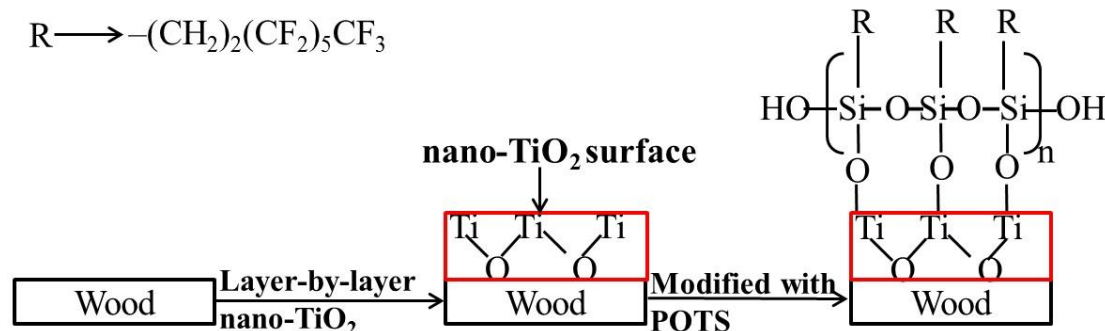


**Fig. 4.** The mechanism of superhydrophobic wood formation

### XRD Pattern

The crystalline phase of TiO<sub>2</sub> nanoparticles deposited on the wood surface was determined by XRD (Fig. 5). The diffraction peaks at 14.7° and 22.6° corresponded to the (101) and (002) planes, respectively, of the characteristic diffraction peaks of cellulose in the wood (Andersson *et al.* 2003). Similarly, the TiO<sub>2</sub> nanoparticles treated wood samples also exhibited obvious cellulose characteristic peaks. The crystallization peaks at 25.5°, 37.7°, 48.2°, 54.4°, and 63.0°, respectively, corresponded to the (101), (004), (200), (105), and (204) crystal planes of anatase TiO<sub>2</sub> (JCPDS card no. 21-1272) (Sun *et al.* 2011; Gao *et al.* 2015b). The new crystallization peaks appearing in the spectrum of the treated wood samples indicated that anatase TiO<sub>2</sub> nanoparticles were deposited on the wood.

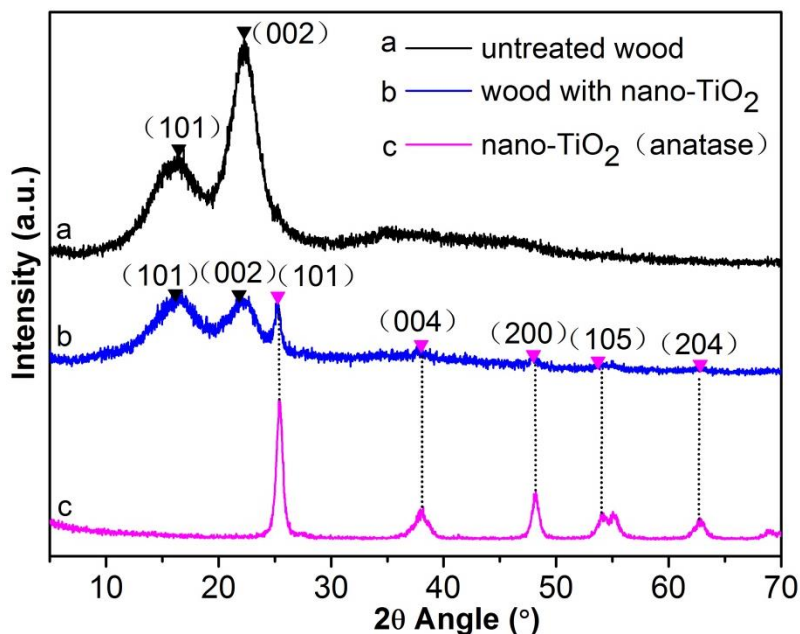


Fig. 5. XRD patterns of: (a) control specimen, (b) treated wood and (c) nano-TiO<sub>2</sub>

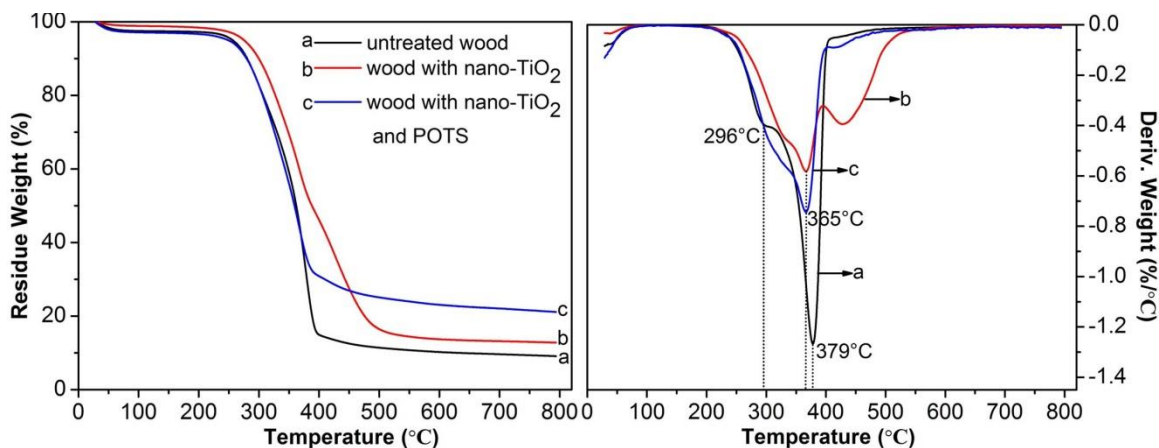
### TG Analysis

Figure 6 shows the TG and DTG curves of untreated wood, wood treated with TiO<sub>2</sub> only, and wood treated with TiO<sub>2</sub> and POTS. Both untreated and treated wood samples showed similar pyrolysis behaviors before 150 °C, which included the evaporation of residual water, physical adsorption moisture, and possible crystal water (Herrera *et al.* 2014). In the TG curve of untreated wood, thermal degradation occurred in three stages. At stage one (193 to 258 °C), water vapor in the wood powder was almost non-existent. The weight loss of about 6.1% with the TG curve closed to a straight line, which was related to the hemicellulose decomposition (Li *et al.* 2014).

Stage two (258 to 391 °C) was the main stage of wood pyrolysis. Small gas molecules and volatile components were produced from larger molecules, mainly due to cellulose degradation accompanied with continuous degradation of lignin, and the weight loss reached 79.3% (Essabir *et al.* 2013). The first shoulder peak and the second strong and sharp endothermic peak at 296 °C and 379 °C, respectively, were attributed to the thermal depolymerisation of hemicellulose and cellulose decomposition (Gao *et al.* 2015a).

The third stage (391 to 800 °C) was the burning carbonization stage. Because the pyrolysis reactions tended to be moderate and wood quality had no significant change to maintain a stable state, the TG curve became a flat straight line again. This stage was associated with the degradation of lignin, tar, and charcoal; the final weight was 9.1% of the original (Yang *et al.* 2007).

The DTG curves of the wood sample with only TiO<sub>2</sub> and the wood sample treated with TiO<sub>2</sub> nanoparticles and POTS showed strong decomposition peaks at 365 °C; the maximum degradation rates were far lower than the untreated wood sample, which may be because TiO<sub>2</sub> nanoparticles formed a protective layer around the wood (Strohm *et al.* 2003). When the specimens were heated to 800 °C at a rate of 10 °C/min, only 9.1% of the original weight remained for the untreated wood sample, 12.8% for the wood sample with TiO<sub>2</sub> nanoparticles, and 21.2% for the wood treated with TiO<sub>2</sub> nanoparticles and POTS. These results confirmed the incorporation of TiO<sub>2</sub> nanoparticles and POTS onto the wood surface.



**Fig. 6.** TG and DTG curves of untreated specimen (a) and specimens assembled with PEI(PSS/TiO<sub>2</sub>)<sub>5</sub> multilayers (b) before and (c) after modification with POTS

### SEM and CA Measurements

The above analysis showed that TiO<sub>2</sub> nanoparticles were successfully deposited on the wood surface and that modified POTS molecules combined with the TiO<sub>2</sub> coating. To study the effects of experimental factors on wood hydrophobicity, the preparation conditions are shown in Table 1. The reaction pH values and self-assembled layers affected the generation of TiO<sub>2</sub> nanoparticles during the LbL assembly process, which was essential for developing the performance of the new products. If the deposit amount is too small, it cannot effectively reflect the nanometer effect of nano-inorganic materials. With more deposits, the interactions between nanomaterials also affects their properties.

The influence of PEI(PSS/TiO<sub>2</sub>)<sub>n</sub> multilayers was studied by SEM of untreated wood at low magnification and treated samples at high magnification (Fig. 7). The micrographs show that wood is a heterogeneous and porous material (sample S0). TiO<sub>2</sub> nanoparticles were present in a random distribution on the wood surface (samples S1 through S5).

The pits were surrounded and partially filled by TiO<sub>2</sub> nanoparticles, suggesting that LbL assembly with TiO<sub>2</sub> nanoparticles did not change the microscopic and macroscopic features of wood. The growth of TiO<sub>2</sub> nanoparticles increased with increasing PEI(PSS/TiO<sub>2</sub>)<sub>n</sub> multilayers when other experimental parameters were unchanged.

Surface wettability was evaluated by CA measurements (Fig. 7). The addition of more self-assembled layers resulted in a larger WCA. Keeping PEI with a pH of 10.5, PSS and TiO<sub>2</sub> nanoparticles with a pH of 6, WCA increased with the increase of the PEI(PSS/TiO<sub>2</sub>)<sub>n</sub> multilayers. The WCAs of S1, S2, S3, S4, and S5 with the corresponding PEI(PSS/TiO<sub>2</sub>)<sub>n</sub> multilayers were 133°, 142°, 153°, 156°, and 161°, respectively. Compared with 31° in the untreated wood (S0), the hydrophobicity was greatly improved. The amount of TiO<sub>2</sub> nanoparticles deposited on the wood surface increased with increasing PEI(PSS/TiO<sub>2</sub>)<sub>n</sub> multilayers, as shown in the EDXA and FTIR spectra (Figs. 2 and 3). Hence, a growing number of POTS molecules combined with TiO<sub>2</sub> nanoparticles on the wood surface, which resulted in increased WCA. When the PEI(PSS/TiO<sub>2</sub>)<sub>n</sub> multilayers reached 5, 7, and 9, the treated wood surface transformed from hydrophilic to superhydrophobic, and the highest WCA reached 161°.

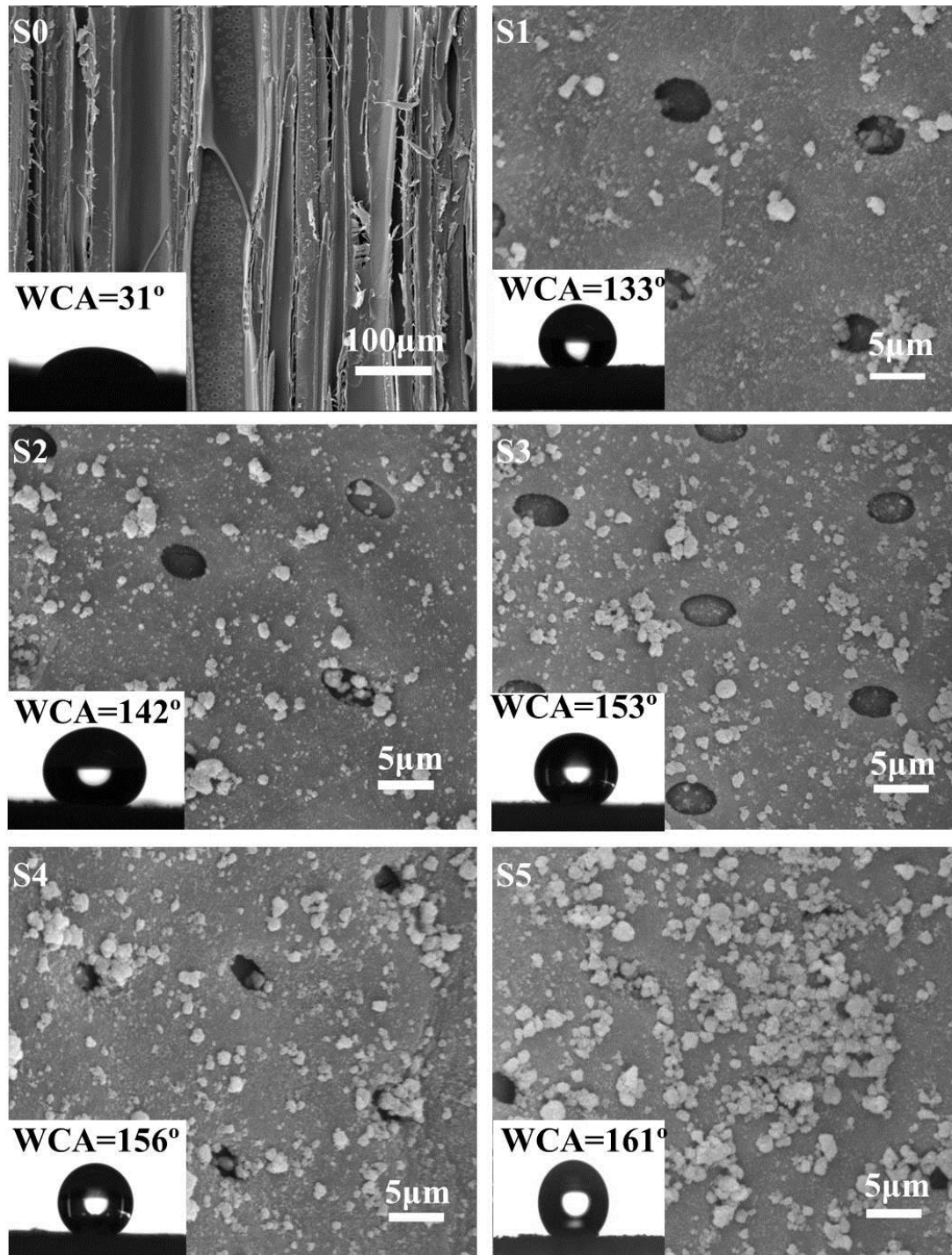


**Fig. 7.** SEM images of control specimen (S0) and specimens assembled with PEI(PSS/TiO<sub>2</sub>)<sub>n</sub> multilayers. S1: n = 1; S2: n = 3; S3: n = 5; S4: n = 7; and S5: n = 9

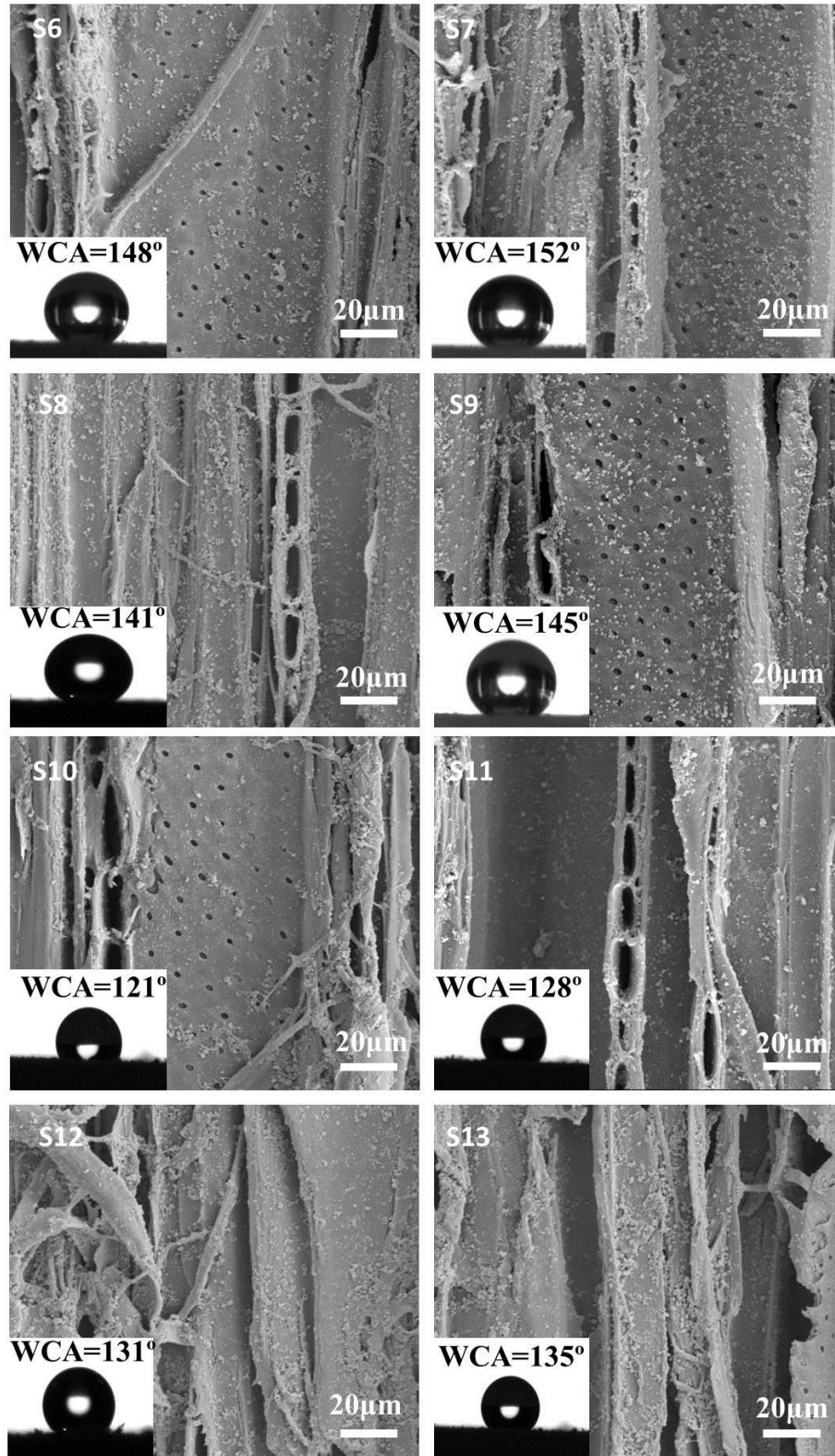


**Fig. 8.** SEM images of specimens assembled with the PEI(PSS/TiO<sub>2</sub>)<sub>5</sub> multilayers at different pH values. S6: pH(PEI) = 10, pH(PSS) = 6, pH(TiO<sub>2</sub>) = 8; S7: pH(PEI) = 10, pH(PSS) = 6, pH(TiO<sub>2</sub>) = 6; S8: pH(PEI) = 10, pH(PSS) = 8, pH(TiO<sub>2</sub>) = 8; S9: pH(PEI) = 10, pH(PSS) = 8, pH(TiO<sub>2</sub>) = 6; S10: pH(PEI) = 6, pH(PSS) = 8, pH(TiO<sub>2</sub>) = 8; S11: pH(PEI) = 6, pH(PSS) = 8, pH(TiO<sub>2</sub>) = 6; S12: pH(PEI) = 6, pH(PSS) = 6, pH(TiO<sub>2</sub>) = 8; and S13: pH(PEI) = 6, pH(PSS) = 6, pH(TiO<sub>2</sub>) = 6

Wood has an anionic characteristic and, thus, can be influenced somewhat by pH. Renneckar and Zhou (2009) reported that in the absence of electrolytes, alkaline pH maximized polymer adsorption for both types of polycations. Thus, the effect of pH on hydrophobicity was examined. The approach of Shiratori and Rubner (2000) has been to use weak polyelectrolytes such as poly(acrylic acid) (PAA) and poly(allylamine hydrochloride) (PAH) whereby control over the layer thickness and molecular organization of an adsorbed polymer chain can be achieved by simple adjustments of the pH of the dipping solutions. In this case, pH controls the linear charge density of an adsorbing polymer as well as the charge density of the previously adsorbed polymer layer. Zhang (2012b) investigated that in acid conditions ( $\text{pH} < 6$ ),  $\text{TiO}_2$  carried a positive charge, while in a basic condition ( $\text{pH}$  from 7 to 11.5),  $\text{TiO}_2$  carried a negative charge. Figure 8 shows SEM images of the treated specimens at the same magnification. The amount of  $\text{TiO}_2$  nanoparticles deposited on the wood surface was different in reactions of different pH. When PEI was in alkaline conditions, *e.g.*, sample S7, more  $\text{TiO}_2$  nanoparticles were deposited on the wood surface.

Figure 8 also shows the WCAs of the treated wood samples. The treated wood samples with PEI fixed at pH 10 showed greater hydrophobicity than the samples with PEI fixed at pH 6. When the pH of PSS and  $\text{TiO}_2$  was changed from 6 to 8, the WCAs of S6, S7, S8, and S9 with PEI at pH 10 were  $148^\circ$ ,  $152^\circ$ ,  $141^\circ$ , and  $145^\circ$ , respectively. WCA decreased with PEI at pH 6, which also indirectly showed that alkaline pH maximized polymer adsorption and that more  $\text{TiO}_2$  nanoparticles were deposited on the wood surface. With PEI fixed at pH 6, the pH values of PSS and  $\text{TiO}_2$  changed from 6 to 8, and the corresponding WCAs of the S10, S11, S12, and S13 treated wood samples were  $121^\circ$ ,  $128^\circ$ ,  $131^\circ$ , and  $135^\circ$ , respectively. The treated wood samples transformed from hydrophilic to hydrophobic when PEI was in alkaline conditions but PSS and  $\text{TiO}_2$  were in acidic conditions. Superhydrophobic wood was achieved when PEI at pH 10 and PSS and  $\text{TiO}_2$  at pH 6.

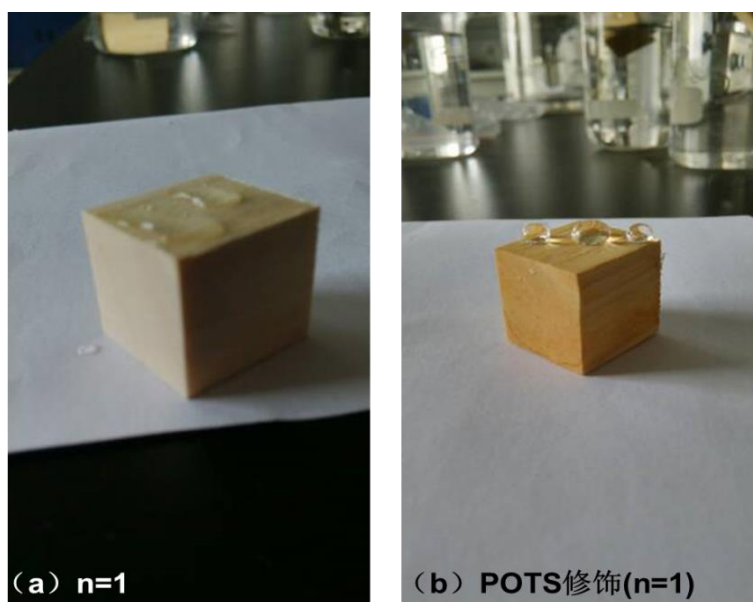


**Fig. 9.** The picture of specimens assembled with  $\text{PEI}(\text{PSS}/\text{TiO}_2)_1$  multilayers (a) before and (b) after modification with POTS contacting with water

Figure 9 shows the picture of specimens assembled with PEI(PSS/TiO<sub>2</sub>)<sub>1</sub> multilayers (a) before and (b) after modification with POTS contacting with water. TiO<sub>2</sub> is a hydrophilic material, so TiO<sub>2</sub>-coated wood surface exhibited hydrophilic characteristics and water droplets quickly seeped into the wood surface. After modification of TiO<sub>2</sub>-coated wood by POTS, the treated wood surface was transformed from hydrophilic to hydrophobic, and the WCA reached about 133° (S1).

In conclusion, Fig. 10 contains a diagram of the LbL assembly technique for fabricating hydrophobic wood. When the surface was covered by a high-surface-roughness film of TiO<sub>2</sub> nanoparticles and subsequently modified by a low-surface-energy thin layer of POTS reagent, wood had a very favorable hydrophobic stability. Thus, functionalized wood surfaces are created by the LbL assembly technique.

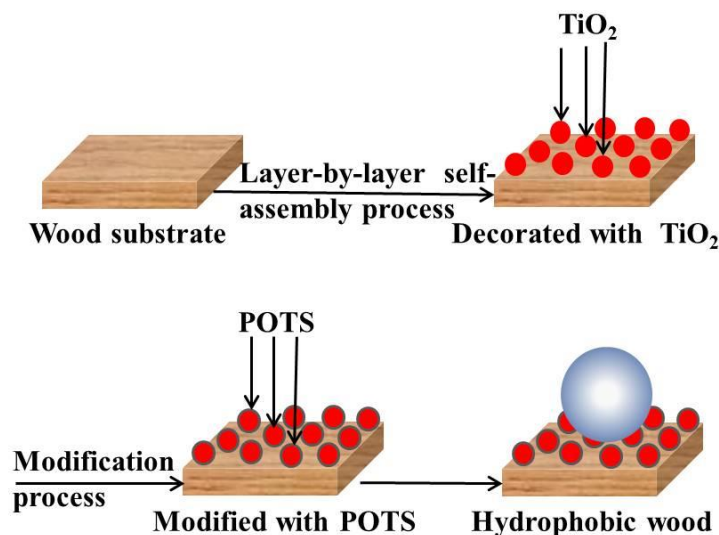


Fig. 10. Schematic for fabricating hydrophobic wood using the LbL assembly technique

### Stability and Durability of Superhydrophobic Wood

The environmental stability and durability of the superhydrophobic wood surface have been investigated (Fig. 11).

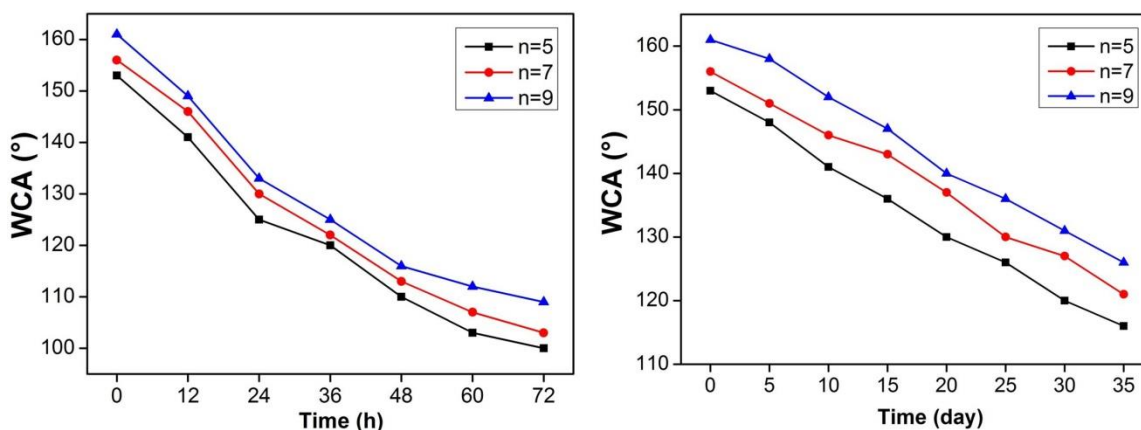


Fig. 11. The environmental stability and durability of the superhydrophobic wood surface assembled with PEI(PSS/TiO<sub>2</sub>)<sub>n</sub> multilayers: n = 5, n = 7, n = 9

The result showed that the WCAs of the prepared wood surfaces still keep their hydrophobicity for a long time in air and the water. Thus, it can be concluded that the superhydrophobic wood had a satisfactory environmental stability and durability.

## CONCLUSIONS

1. A superhydrophobic wood surface was fabricated in two steps. First, a high-surface-roughness film of TiO<sub>2</sub> nanoparticles was deposited on the wood surface by the layer-by-layer (LbL) assembly technique, and next, a low-surface-energy thin layer was coated on the TiO<sub>2</sub> nanoparticles with the 1H,1H, 2H,2H-perfluoroalkyltriethoxysilane (POTS) surface modifying agent.
2. The influence of experimental factors, such as the reaction pH values and self-assembled layers on the wood surface, was investigated; samples were obtained at different preparation conditions of the LbL assembly process. Larger water contact angle (WCA) was achieved when PEI was maintained in alkaline conditions, PSS and TiO<sub>2</sub> were maintained in acidic conditions, and more multilayers were added.
3. After the superhydrophobic treatment, the wettability of the wood surface was transformed from hydrophilic to superhydrophobic with the highest WCA of 161°.
4. A simple, facile, novel, and feasible procedure for fabricating superhydrophobic wood was developed and nanoscale films on wood surfaces were created by the LbL assembly technique.

## ACKNOWLEDGMENTS

This project was supported by the National Natural Science Foundation of China (31170516, 31470581) and the Fundamental Research Funds for the Central Universities (DL12EB03).

## REFERENCES CITED

- Agarwal, M., Xing, Q., Shim, B. S., Kotov, N., Varahramyan, K., and Lvov, Y. (2009). "Conductive paper from lignocellulose wood microfibers coated with a nanocomposite of carbon nanotubes and conductive polymers," *Nanotechnology* 20(21), 9431-9431. DOI: 10.1088/0957-4484/20/21/215602
- Andersson, S., Serimaa, R., Paakkari, T., Saranpää, P., and Pesonen, E. (2003). "Crystallinity of wood and the size of cellulose crystallites in Norway spruce (*Picea abies*)," *J. Wood Sci.* 49 (6), 531-537. DOI: 10.1007/s10086-003-0518-x
- Chandrasekhar, H. R., Chandrasekhar, M., and Manghnani, M. H. (1980). "Phonons in TiO<sub>2</sub>-SiO<sub>2</sub> glasses," *J. Non-Cryst. Solids* 40(1), 567-575. DOI: 10.1016/0022-3093(80)90130-1
- Colomer, M. T., and Velasco, M. J. (2007). "Rutile-type dense ceramics fabricated by pressureless sintering of Ti<sub>1-x</sub>Ru<sub>x</sub>O<sub>2</sub> powders prepared by sol-gel," *J. Eur. Ceram. Soc.* 27(6), 2369-2376. DOI: 10.1016/j.jeurceramsoc.2006.09.006

- Cranston, E., and Gray, D. (2006). "Formation of cellulose-based electrostatic layer-by-layer films in a magnetic field," *Sci. Technol. Adv. Mat.* 7 (4) 319-321.  
DOI: 10.1016/j.stam.2006.02.007
- Dai, S., Zhang, D., Shi, Q., Han, X., Wang, S., and Du, Z. (2013). "Biomimetic fabrication and tunable wetting properties of three-dimensional hierarchical ZnO structures by combining soft lithography templated with lotus leaf and hydrothermal treatments," *Cryst. Eng. Comm.* 15(27), 5389-5576. DOI: 10.1039/C3CE40238J
- Decher, G. (1997). "Fuzzy nanoassemblies: Toward layered polymeric multicomposites," *Science* 277 (5330), 1232-1237. DOI: 10.1126/science.277.5330.1232
- Elosua, C., Torres, D., Hernaez, M., Matias, I., and Arregui, F. (2013). "Comparative study of layer-by-layer deposition technique for poly(sodium phosphate) and poly(allylamine hydrochloride)," *Nanoscale Res. Lett.* 8(1) 539-545.  
DOI: 10.1186/1556-276X-8-539
- Essabir, H., Hilali, E., Elgharad, A., El, Minor H., Imad, A., Elamraoui, A., and Al Gaoudi, O. (2013). "Mechanical and thermal properties of bio-composites based on polypropylene reinforced with nut-shells of argan particles," *Mater. Design* 49, 442-448. DOI: 10.1016/j.matdes.2013.01.025
- Fang, F., Zhang, X., Meng, Y., Gu, Z., Bao, C., Ding, X., Li, S., Chen, X., and Tian, X. (2015). "Intumescent flame retardant coatings on cotton fabric of chitosan and ammonium polyphosphate via layer-by-layer assembly," *Surf. Coat. Tech.* 262, 9-14.  
DOI: 10.1016/j.surfcoat.2014.11.011
- Gao, L., Lu, Y., Zhan, X., Li, J., and Sun, Q. (2015a). "A robust, anti-acid, and high-temperature-humidity-resistant superhydrophobic surface of wood based on a modified TiO<sub>2</sub> film by fluoroalkyl silane," *Surf. Coat. Tech.* 262, 33-39.  
DOI:10.1016/j.surfcoat.2014.12.005
- Gao, L., Zhan, X., Lu, Y., Li, J., and Sun, Q. (2015b). "pH-dependent structure and wettability of TiO<sub>2</sub>-based wood surface," *Mater. Lett.* 142, 217-220.  
DOI: 10.1016/j.matlet.2014.12.035
- Herrera, R., Erdocia, X., Llano-Ponte, R., and Labidi, J. (2014). "Characterization of hydrothermally treated wood in relation to changes on its chemical composition and physical properties," *J. Anal. Appl. Pyrol.* 107(9), 256-266.  
DOI: 10.1016/j.jaap.2014.03.010
- Laufer, G., Kirkland, C., Morgan, A., and Crunlan, C. (2012). "Intumescent multilayer nanocoating, made with renewable polyelectrolytes, for flame-retardant cotton," *Biomacromolecules* 13(9), 2843-2848. DOI: 10.1021/bm300873b
- Li, H., Fu, S., and Peng, L. (2013). "Surface modification of cellulose fibers by layer-by-layer self-assembly of lignosulfonates and TiO<sub>2</sub> nanoparticles: Effect on photocatalytic abilities and paper properties," *Fiber. Polym.* 14(11), 1794-1802.  
DOI: 10.1007/s12221-013-1794
- Li, X., Lei, B., Lin, Z., Huang, L., Tan, S., and Cai, X. (2014). "The utilization of bamboo charcoal enhances wood plastic composites with excellent mechanical and thermal properties," *Mater. Design* 53(2014), 419-424.  
DOI:10.1016/j.matdes.2013.07.028
- Lin, Z., Renneckar, S., and Hindman, D. P. (2008). "Nanocomposite-based lignocellulosic fibers 1. Thermal stability of modified fibers with clay-polyelectrolyte multilayers," *Cellulose* 15 (2), 333-346. DOI: 10.1007/s10570-007-9188-y
- Lu, Z., Eadula, S., Zheng, Z., Xu, K., Grozdits, G. and Lvov, Y. (2007). "Layer-by-layer nanoparticle coatings on lignocelluloses wood microfibers," *Colloid Surface A-*

- Physicochem. Eng. Asp.* 292(1), 56-62. DOI: 10.1016/j.colsurfa.2006.06.008
- Marais, A., Utsel, S., Gustafsson, E. and Wågberg, L. (2014). "Towards a superstrainable paper using the layer-by-layer technique," *Carbohydr. Polym.* 100(2), 218-224. DOI: 10.1016/j.carbpol.2013.03.049
- Razmjou, A., Arifin, E., Dong, G., Mansouri, J., and Chen, V. (2012). "Superhydrophobic modification of TiO<sub>2</sub> nanocomposite PVDF membranes for applications in membrane distillation," *J. Membrane Sci.* 415(10), 850-863. DOI: 10.1016/j.memsci.2012.06.004
- Rennekar, S., and Zhou, Y. (2009). "Nanoscale coatings on wood: Polyelectrolyte adsorption and layer-by-layer assembled film formation," *ACS Appl. Mater. Interfaces* 1(3), 559-566. DOI: 10.1021/am800119q
- Shiratori, S., and Rubner, M. (2000). "pH-dependent thickness behavior of sequentially adsorbed layers of weak polyelectrolytes," *Macromolecules* 33(11), 4213-4219. DOI: 10.1021/ma991645q
- Strohm, H., Sgraja, M., Bertling, J., and Löbmann, P. (2003). "Preparation of TiO<sub>2</sub>-polymer hybrid microcapsules," *J. Mater. Sci.* 38(8), 1605-1609. DOI: 10.1023/A:1023294719482
- Sun, Q., Lu, Y., and Liu, Y. (2011). "Growth of hydrophobic TiO<sub>2</sub> on wood surface using a hydrothermal method," *J. Mater. Sci.* 46(24), 7706-7712. DOI: 10.1007/s10853-011-5750-y
- Wan, C., Lu, Y., Sun, Q., and Li, J. (2014). "Hydrothermal synthesis of zirconium dioxide coating on the surface of wood with improved UV resistance," *Appl. Surf. Sci.* 321, 38-42. DOI: 10.1016/j.apsusc.2014.09.135
- Wang, C., Piao, C., and Lucas, C. (2011a). "Synthesis and characterization of superhydrophobic wood surfaces," *J. Mater. Sci.* 119(3), 1667-1672. DOI: 10.1002/app. 32844.
- Wang, S., Liu, C., Liu, G., Zhang, M., Li, J., and Wang, C. (2011b). "Fabrication of superhydrophobic wood surface by a sol-gel process," *Appl. Surf. Sci.* 258(2), 806-810. DOI:10.1016/j.apsusc.2011.08.100
- Wang, S., Shi, J., Liu, C., Xie, C., and Wang, C. (2011c). "Fabrication of a superhydrophobic surface on a wood substrate," *Appl. Surf. Sci.* 257(22), 9362-9365. DOI: 10.1016/j.apsusc.2011.05.089
- Wang, Y., Wang, L., Wang, S., Wood, R.J., and Xue, Q. (2012). "From natural lotus leaf to highly hard-flexible diamond-like carbon surface with superhydrophobic and good tribological performance," *Surf. Coat. Tech.* 206(8-9), 2258-2264. DOI: 10.1016/j.surfcoat.2011.10.001
- Xing, Q., Eadula, S., and Lvov, Y. (2007). "Cellulose fiber-enzyme composites fabricated through layer-by-layer nanoassembly," *Biomacromolecules* 8(6), 1987-1991. DOI: 10.1021/bm070125x
- Yang, H., Yan, R., Chen, H., Lee, D. H., and Zheng, C. (2007). "Characteristics of hemicellulose, cellulose and lignin pyrolysis," *Fuel* 86(12-13), 1781-1788. DOI: 10.1016/j.fuel.2006.12.013
- Zamarreño, C. R., Hernaez, M., Sanchez, P., Del Villar, I., Matias, R., and Arregui, F. J. (2011). "Optical fiber humidity sensor based on lossy mode resonances supported by TiO<sub>2</sub>/PSS coatings," *Procedia Eng.* 25, 1385-1388. DOI:10.1016/j.proeng.2011.12.342

- Zhang, L., Gong, F., Zhao, Q., and Ma, J. (2012b). "Impact of zeta potential and particle size on TiO<sub>2</sub> nanoparticles' coagulation," *Int. J. Civ. Eng. Struct.* 1(1), DOI: 10.5729/igces.vol1.issue1.93
- Zhang, M., Wang, S., Wang, C., and Li, J. (2012a). "A facile method to fabricate superhydrophobic cotton fabrics," *Appl. Surf. Sci.* 261(19), 561-566. DOI: 10.1016/j.apsusc.2012.08.055
- Zhang, X., Shi, F., Yu, X., Liu, H., Fu, Y., Wang, Z., Jiang, L., and Li, X. (2004). "Polyelectrolyte multilayer as matrix for electrochemical deposition of gold clusters: Toward super-hydrophobic surface," *J. Am. Chem. Soc.* 126(10), 3064-3065. DOI: 10.1021/ja0398722
- Zheng, R., Tshabalala, M., Li, Q., and Wang, H. (2015). "Construction of hydrophobic wood surfaces by room temperature deposition of rutile (TiO<sub>2</sub>) nanostructures," *Appl. Surf. Sci.* 328, 453-458. DOI: 10.1016/j.apsusc.2014.12.083
- Zhou, Y., Renneckar, S., Pillai, K., Li, Q., Lin, Z., and Church, W. T. (2010). "Layer-by-layer bondlines for macroscale adhesion," *BioResources* 5(3), 1530-1541. DOI: 10.15376/biores.5.3.1530-1541

Article submitted: December 13, 2015; Peer review completed: March 17, 2016; Revised article received and accepted: March 28, 2016; Published: April 6, 2016.  
DOI: 10.15376/biores.11.2.4605-4620